

Cyclostationary Detection of Cognitive Radio Systems using GFDM Modulation

Dorin Panaitopol^a, Rohit Datta^b and Gerhard Fettweis^b

^aNEC Technologies (UK), FMDC Lab., ComTech Department, Nanterre, France.

^bVodafone Chair Mobile Communications Systems, Dresden University of Technology, Dresden, Germany.

Email: dorin.panaitopol@nectech.fr, {rohit.datta, gerhard.fettweis}@ifn.et.tu-dresde.de

Abstract—A cognitive radio should be able to detect unused spectrum band and to change its transmission parameters in order to transmit within these free bands. To achieve this, reliable detection of incumbent signals as well as of other opportunistic signals that are using the said spectrum, is necessary. Generalized Frequency Division Multiplexing (GFDM) is a recent multicarrier modulation technique with extremely low out-of-band radiation that makes it an attractive choice for the PHY layer of cognitive radio. GFDM has an innovative tail biting cyclic prefix which shows unique circular detection properties. In this paper, we consider the cyclostationarity properties of GFDM and compare this with well studied OFDM. Detection of GFDM based opportunistic signal by cyclostationary detection is shown and compared to OFDM detection by the same method.

I. INTRODUCTION

Radio spectrum is one of the most scarce resources in wireless communication. With proliferation of large screen smart wireless devices, innovative services and growing number of mobile users, the demand for radio spectrum has made this scarcity more stark. To cope with this, regulatory bodies such as the Federal Commission for Communication (FCC) in USA, or the Electronic Communications Committee within the European Conference of Postal and Telecommunications Administrations (ECC CEPT) in Europe, have recently published requirements in the scope of finalizing rules to make the unused spectrum in the TV bands available for unlicensed broadband wireless devices [1], [2]. Spectrum utilization at any given location, frequency and time is highly inefficient [3]. Hence, interest in allowing opportunistic users to access licensed spectrum has been tremendously growing among regulatory bodies (e.g. FCC in USA and Ofcom in UK) and standardization groups such as IEEE802.16h, IEEE802.11af, P1900.4a etc.

Opportunistic access in licensed frequency bands should be controlled such that they do not create any harmful interference to legacy primary licensed users and hence novel PHY designs have been identified as a key requirement of cognitive radio. Opportunistic users will be allowed to transmit data over the frequency spectrum when incumbent users or other opportunistic users are inactive. The opportunistic PHY should be extremely sensitive, to detect even the weakest incumbent signal.

In the recent 2010 FCC and Ofcom ruling, a geo-location database query mechanism for the protection of incumbent users was proposed and they eliminated the requirements of

spectrum sensing [4], [5]. Geo-location databases store information about the incumbent users at a particular location and opportunistic users guarantee that they communicate in white spaces and hence provide necessary protection to incumbent users. However, protection of other opportunistic users using the same frequency bands is still an open question. A number of spectrum sensing algorithms have been proposed, each algorithm has its own operational requirements, advantages and disadvantages; a comprehensive survey has recently been published by Yucek et al [6]. However, all current sensing algorithms focus on the detection of incumbent user signals only.

The multiband Generalized Frequency Division Multiplexing (GFDM) is a relatively new idea for designing a multicarrier PHY [7], [8]. GFDM is well suited for cognitive radio as the choice of pulse shaping filters makes the out-of-band leakage extremely small. Compared to orthogonal frequency division multiplexing (OFDM), which has rectangular pulse shaping, GFDM with root-raised cosine (RRC) transmit pulse shaping causes lesser interference to the adjacent incumbent frequency bands. Another feature of GFDM is a tail biting cyclic prefix (CP). This feature is useful in cyclostationary detection. To provide necessary protection to opportunistic users, the GFDM signal needs to be sensed reliably, so that no other opportunistic cognitive radio signal is transmitted when GFDM signal is occupying the frequency band.

In this paper, we use spectrum sensing for the protection of opportunistic users and assumed incumbent users are protected using geo-location database approach. More complex than the classical Energy Detector (ED) [9], the Cyclostationary Detector (CD) [10], [11] is a detector which is exploiting cyclostationary features of the signal. GFDM being a newly designed cognitive radio PHY modulation scheme, cyclostationary properties of GFDM have not been described till now. For the first time ever, in this paper we graphically represent the Cyclostationary Autocorrelation Function (CAF) of both OFDM and GFDM signals. Then, we apply the Generalized Likelihood Ratio Test (GLRT) [10] for one non-zero cyclic frequency which is characterizing the OFDM/GFDM CAF structure and is differentiating it from noise [12]. The numerical results show a comparison between ED and CD using GLRT, for both OFDM and GFDM signals.

The rest of the paper is organized as follows. In Section II, the OFDM and GFDM transmission models are described.

While Section III presents the second order cyclostationary properties of both OFDM and GFDM signals, Section IV briefly describes ED and CD detectors which are further used for the numerical results provided by Section V. The paper ends with the conclusions provided by Section VI.

As the main focus of the paper is about sensing GFDM and OFDM transmitted signals using cognitive radio hardware, the GFDM and OFDM receiver structures are not explained here, but are explained in details in [7], [8].

II. SIGNAL TRANSMISSION MODEL

Section II deals with the description of the transmitted signal model of both OFDM (i.e., subsection II-A) and GFDM (i.e., subsection II-B) modulations.

A. OFDM Transmission

This section details the OFDM transmitter [7]. The input data stream is modulated by a QAM modulator resulting in a complex symbol stream $d[\ell]$, $\ell = 0, 1, \dots, K-1$. This stream is passed through the serial-to-parallel converter, whose output is a set of K parallel QAM symbols. Inverse DFT on these symbols is efficiently implemented using the IFFT algorithm. This yields the OFDM symbol according to

$$x[n] = \frac{1}{\sqrt{K}} \sum_{k=0}^{K-1} d[k] e^{j2\pi kn/K}, \quad 0 \leq n \leq K-1. \quad (1)$$

The above sequence corresponds to the samples of the signal. Each sample is made up of sum of QAM symbols $d[k]$ each modulated by $e^{j2\pi kn/K}$, $k = 0, 1, \dots, K-1$.

The cyclic prefix is then added to the OFDM symbol to obtain $\tilde{x}[n]$. This is then passed through a D/A converter, resulting in the baseband OFDM signal $x_{OFDM}(t)$.

B. GFDM Transmission

GFDM is a multi-carrier modulation scheme with flexible pulse shaping. Initially the binary data is modulated and divided into sequences of $K \times M$ complex valued data symbols. Each such sequence $d[\ell]$, $\ell = 0, 1, \dots, KM-1$, is spread across K subcarriers and M time slots for transmission. The data is represented by means of a block structure defined in equation (2) as

$$\mathbf{D} = [\mathbf{d}_0, \mathbf{d}_1 \dots \mathbf{d}_{K-1}]^T, \\ = \begin{bmatrix} d_0[0] & \dots & d_0[M-1] \\ \vdots & & \vdots \\ d_{K-1}[0] & \dots & d_{K-1}[M-1] \end{bmatrix}, \quad (2)$$

where $d_k[m] \in \mathbb{C}$ is the data symbol transmitted on the k th subcarrier and in the m th time slot. OFDM is a special case of GFDM, where $M = 1$, i.e. the data is spread only across frequencies and not in time.

The GFDM transmitter structure is shown in Fig. 1. In the k th branch of the transmitter, the complex data symbols $d_k[m]$,

$m = 0, \dots, M-1$ are upsampled by factor N , resulting in

$$d_k^N[n] = \sum_{m=0}^{M-1} d_k[m] \delta[n - mN], \quad n = 0, \dots, NM-1, \quad (3)$$

where $\delta[\cdot]$ is the Dirac delta function. Consequently, $d_k^N[mN] = d_k[m]$ and $d_k^N[n] = 0$ for $n \neq mN$.

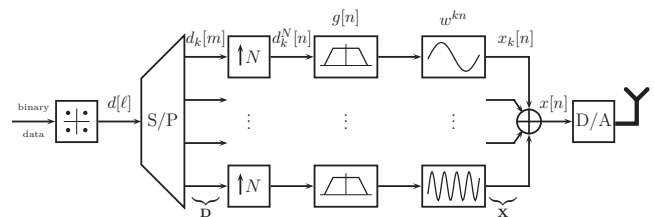


Fig. 1. GFDM transmitter system model

The pulse shaping filter $g[n]$ is applied to the sequence $d_k^N[n]$, followed by digital subcarrier upconversion. The resulting subcarrier transmit signal $x_k[n]$ can be mathematically expressed as

$$x_k[n] = (d_k^N \otimes g)[n] \cdot w^{kn} \quad (4)$$

where \otimes denotes circular convolution and $w^{kn} = e^{j\frac{2\pi}{N}kn}$. Similar to equation (2), the transmit signals can be expressed in a block structure

$$\mathbf{X} = [\mathbf{x}_0, \mathbf{x}_1 \dots \mathbf{x}_{K-1}]^T, \\ = \begin{bmatrix} x_0[0] & \dots & x_0[MN-1] \\ \vdots & & \vdots \\ x_{K-1}[0] & \dots & x_{K-1}[MN-1] \end{bmatrix} \quad (5)$$

The transmit signal for a data block \mathbf{D} is then obtained by summing up all subcarrier signals according to

$$x[n] = \sum_{k=0}^{K-1} x_k[n]. \quad (6)$$

For the ease of equalization at the receiver, a cyclic extension is appended to $x[n]$ to obtain $\tilde{x}[n]$. Tail biting [13], has been applied to GFDM [7], [8] and this has been used to reduce the length of the CP. It is used to maintain the circular structure within each block.

This tail biting concept exploits the digital implementation of the filters to perform circular convolution. $\tilde{x}[n]$ is then passed to the digital-to-analog converter and finally $x_{GFDM}(t)$ is sent over the channel.

III. OFDM AND GFDM CYCLOSTATIONARY PROPERTIES

The autocorrelation function $R_{rr}(t, \tau)$ of the received signal $r(t)$ (where $r(t) = x_{OFDM}(t) + n(t)$ or $r(t) = x_{GFDM}(t) + n(t)$, with $n(t)$ the white additive Gaussian noise) can be represented by Fourier series expansion as

$$R_{rr}(t, \tau) = \sum_{\alpha \in \psi} R_{rr}^{\alpha}(\tau) \exp(j2\pi\alpha t), \quad (7)$$

where α is a cyclic frequency, ψ is the entire set of cyclic frequencies, and $R_{rr}^\alpha(\tau)$ is the Fourier coefficient, also called Cyclic Autocorrelation Function (CAF). The CAF of the second order autocorrelation function can be written as

$$\begin{aligned} R_{rr}^\alpha(\tau) &= \lim_{T \rightarrow \infty} \frac{1}{T} \int_{-\frac{T}{2}}^{\frac{T}{2}} r(t)r^*(t-\tau) \exp(-j2\pi\alpha t) dt \\ &= \lim_{T \rightarrow \infty} \frac{1}{T} \int_{-\frac{T}{2}}^{\frac{T}{2}} r^*(t)r(t+\tau) \exp(-j2\pi\alpha t) dt. \end{aligned} \quad (8)$$

The expression described by (8) could be time-discrete approximated by

$$R_{rr}^\alpha(d) = \frac{1}{N_r} \sum_{n=0}^{N_r-1} r^*(n)r(n+d) \exp(-j2\pi\alpha n\Delta t), \quad (9)$$

where d represents the delay time normalized by the sampling period Δt , and N_r is the total received number of samples. Equation (9) is further used throughout the paper for the graphical representation of the GFDM cyclostationary properties.

As it will be seen later, the cyclostationary properties of both OFDM and GFDM signals are given by the cyclic prefix and useful symbol length. The cyclic prefix construction is graphically presented in Fig. 2 and Fig. 3. In Fig. 2 we have therefore represented an example with 3 OFDM symbols. We have also defined $T_{U,OFDM}$ as the useful symbol period, $T_{CP,OFDM}$ as the cyclic prefix period and $T_{S,OFDM} = T_{U,OFDM} + T_{CP,OFDM}$ as the OFDM symbol period.

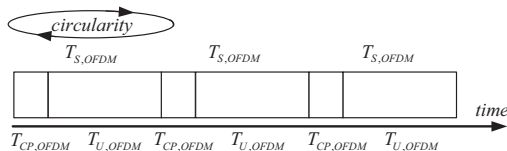


Fig. 2. OFDM structure - example with 3 OFDM symbols

Similar to Fig. 2, in Fig. 3 we have represented a single GFDM symbol with $N_s = 3$ useful payloads. It can be noticed that the total GFDM symbol period $T_{S,GFDM}$, which consists of a cyclic prefix period $T_{CP,GFDM}$ and a useful symbol period $T_{U,GFDM}$, can also be expressed in terms of OFDM parameters. The example from Fig. 3 corresponds to a situation where $T_{S,GFDM} = T_{CP,GFDM} + N_s \cdot T_{U,OFDM}$, with $N_s = 3$ as mentioned earlier.

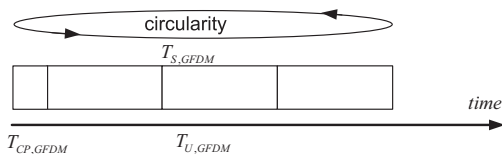


Fig. 3. GFDM structure - example with 1 GFDM symbol and $N_s = 3$ useful payloads

Further, Fig. 4 shows the CAF of an OFDM signal with $T_{CP,OFDM} = T_{U,OFDM}/4$. Similarly, a GFDM modulation

with $T_{CP,GFDM} = T_{U,OFDM}/4$ and $N_s = 16$ is represented in Fig. 5. Please notice that the cyclic frequencies are at multiple of $1/T_{S,OFDM}$ and $1/T_{S,GFDM}$ respectively, and the peaks are encountered at delays equal to $T_{U,OFDM}$ and $T_{U,GFDM}$ respectively. However, unlike OFDM, GFDM exhibits extra side crossing peaks (see Fig. 5).

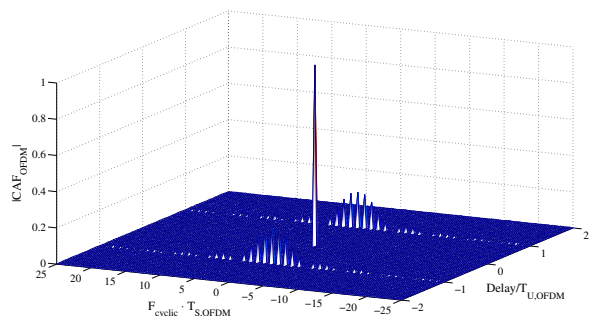


Fig. 4. CAF of OFDM, with $T_{CP,OFDM} = T_{U,OFDM}/4$

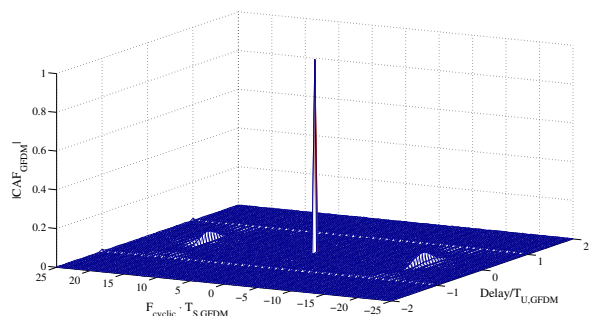


Fig. 5. CAF of GFDM, with $T_{CP,GFDM} = T_{U,OFDM}/4$ and $N_s = 16$

In Fig. 6 we increased the circularity of the signal by increasing the CP. The time period of the CP is now $T_{CP,GFDM} = T_{U,GFDM}/4$. Please note that we have now reached the same peak amplitude as in Fig. 4. However, extra side peaks are still present.

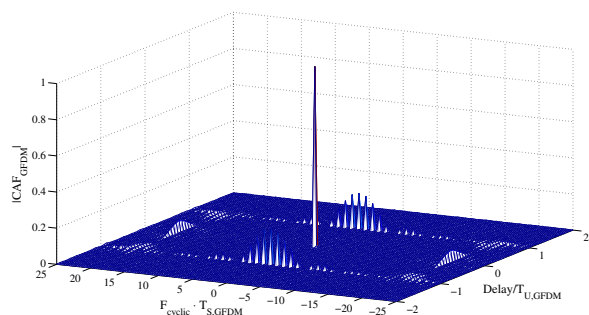


Fig. 6. CAF of GFDM, with $T_{CP,GFDM} = T_{U,GFDM}/4$ and $N_s = 16$

Further, Fig. 7 and Fig. 8 are zoomed in representations of Fig. 6.

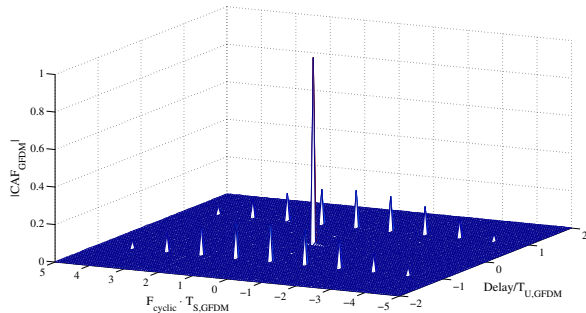


Fig. 7. Zoom on CAF (around the cyclic frequency 0) - for GFDM with $T_{CP,GFDM} = T_{U,GFDM}/4$ and $N_s = 16$

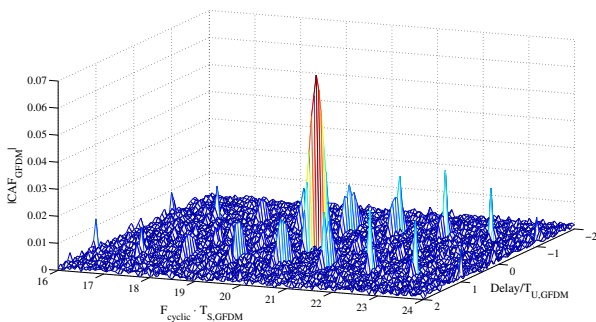


Fig. 8. Zoom on CAF (around the cyclic frequency $20/T_{S,GFDM}$) - for GFDM with $T_{CP,GFDM} = T_{U,GFDM}/4$ and $N_s = 16$

IV. CLASSICAL DETECTORS

This short section is dedicated to the energy detector and to the cyclostationary detector further used in Section V.

A. Energy Detector

Energy detection is a well known detection method [9] which consists of two parts: an energy computation block and a comparison block. The threshold used in the comparison block is chosen according to a desired false alarm probability $P_{FA,target}$ and is given by

$$\gamma = \frac{\sqrt{2}}{\sqrt{N_r}} \sigma_n^2 Q^{-1} \{P_{FA,target}\} + \sigma_n^2, \quad (10)$$

where N_r is the number of samples of the digital signal and σ_n^2 is the noise variance. We denote by Q^{-1} the inverse of the Q function [14].

The weakness of the ED is that a wrong computed threshold value is affecting both the detection probability P_D and the real false alarm probability $P_{FA,real}$, which differs from the $P_{FA,target}$. Therefore ED is very sensitive to noise uncertainty: if the noise is not correctly estimated, ED is said to be uncertain.

B. Generalized Cyclostationary Detector

The Generalized Likelihood Ratio Test (GLRT) algorithm for cyclostationary detection is computing the covariance matrix $\sum_r(\alpha)$ [10]. Based on this covariance matrix, the method further computes a test statistic $N_r \cdot r_{rr}^\alpha(\tau) \cdot (\sum_r(\alpha))^{-1} \cdot r_{rr}^\alpha(\tau)^T$, where $r_{rr}^\alpha(\tau) = [Re(R_{rr}^\alpha(\tau)), Im(R_{rr}^\alpha(\tau))]$. The test statistic is then compared with a threshold γ , which is computed with the help of the following equation:

$$P_{FA,target} = 1 - \Gamma(1, \gamma/2), \quad (11)$$

where Γ is the incomplete gamma function. Similarly to ED (see equation (10)), the threshold γ can be therefore expressed as a function of $P_{FA,target}$.

V. NUMERICAL RESULTS

The simulation further considers 10 ms signal duration for both OFDM and GFDM. In Fig. 9 we have represented the detection probability in terms of SNR (i.e., the ratio between received signal power and noise power). For OFDM, simulations consider an IFFT length of 128, useful symbol period $T_{U,OFDM} = 4.256 \mu s$, and cyclic prefix period $T_{CP,OFDM} = T_{U,OFDM}/4$. For GFDM, the root raised cosine coefficient is 0.3, and the number of useful payloads is $N_s = 16$. The sampling time is $4.256/128 \mu s$ for both GFDM and OFDM.

Please also note that, for GFDM, one simulation corresponding to a higher detection probability considers $T_{CP,GFDM} = T_{U,GFDM}/4$ (see the "circle" curve from Fig. 9), and the other simulation corresponding to a lower detection probability considers $T_{CP,GFDM} = T_{CP,OFDM}$ (see the "diamond" curves Fig. 9).

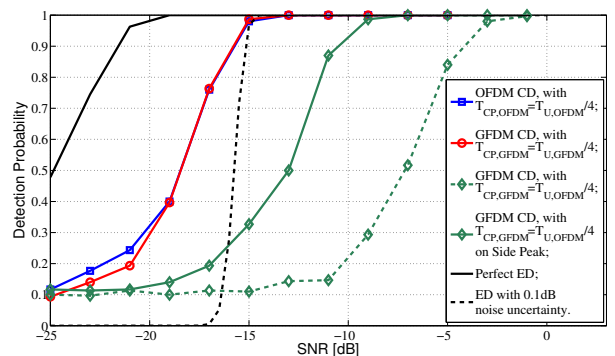


Fig. 9. Detection Probability in terms of SNR - Comparison between Energy and Cyclostationary Detectors for 10 ms OFDM and GFDM signals, for $P_{FA,target} = 0.1$ and different cyclic prefix lengths

Please note that all detectors used for comparison purposes in Fig. 9 have been configured for a target false alarm probability $P_{FA,target} = 0.1$. Multiple tests have been made on perfect (i.e., 0 dB noise uncertainty) and less accurate ED with noise uncertainty 0.1 dB, and CD using the cyclic peaks at the cyclic positions $1/T_{S,OFDM}$ and $1/T_{S,GFDM}$ respectively. Simulation results therefore, show that the GFDM

cyclostationary detection is still reliable when it is sharing the same amount of "circularity" as the OFDM signals (i.e., the sum of all cyclic prefixes is the same). As shown in Fig. 9, CD outperforms ED when the latter is affected by a certain noise estimation uncertainty (i.e., 0.1 dB for our simulations).

Fig. 9 also shows that when GFDM CP is low, cyclostationary properties can still be recovered by using the position of one side peak (see the "diamond" continuous curve from Fig. 9). This interesting aspect gives another important advantage to GFDM which is now able to use smaller CP, and hence, increases the total transmitted throughput.

VI. CONCLUSIONS

The work presented in this paper is analyzing and evaluating the sensing characteristics of the new cognitive radio physical layer modulation scheme called GFDM. GFDM is an extremely attractive multi carrier modulation scheme suitable for cognitive radio PHY, as it has a low out-of-band radiation into the adjacent frequency bands. It is extremely important, that, to maintain regulatory quality of service, cognitive radios reliably detect not only incumbent active transmissions, but also other opportunistic signals. GFDM with its special tail biting construction of the cyclic prefix has remarkable cyclostationary properties, which are used here to detect GFDM signal. In this work, cyclostationary properties of OFDM are compared to that of GFDM. Simulations show that when the sum of all cyclic prefixes is the same, for both OFDM and GFDM signals, the cyclostationary detection performance is similar. However, this occurs only when the CD is configured to the cyclic frequencies obtained from the circular symbol structure, which was initially inspired by OFDM. As a matter of fact, for certain scenarios when the cyclic prefix is sufficiently low, it seems worthy to use the side peaks positions which are characteristic only to GFDM. Finally, CD and ED performances are also compared for these two modulations.

ACKNOWLEDGEMENT

The research leading to these results was derived from the European Community Seventh Framework Program (FP7) under Grant Agreement number 248454 (QoS MOS).

REFERENCES

- [1] FCC, "Notice of Proposed Rule-making, in the matter of unlicensed operation in the TV broadcast bands (ET Docket No. 04-186) and additional spectrum for unlicensed devices below 900 Mhz and in the 3 Ghz band (ET DocketNo. 02-380)," FCC, Tech. Rep. 04-113, 2004.
- [2] ECC, "Technical and Operational Requirements for the Possible Operation of Cognitive Radio Systems in the "White Spaces" of the Frequency Band 470-790 Mhz," CEPT, Tech. Rep. 159, Jan 2011.
- [3] K. Arshad, M. A. Imran, and K. Moessner, "Collaborative Spectrum Sensing Optimisation Algorithms for Cognitive Radio Networks," *International Journal of Digital Multimedia Broadcasting*, vol. 2010, pp. 1-20, 2010.
- [4] Federal Communications Commission: Second Memorandum Opinion and Order, Tech. Rep. 10-174, September 2010. [Online]. Available: <http://www.fcc.gov/>
- [5] Ofcom, "Implementing geolocation," Office of Communications, Tech. Rep., December 2010.
- [6] T. Yucek and H. Arslan, "A Survey of Spectrum Sensing Algorithms for Cognitive Radio Applications," *IEEE Communications Surveys & Tutorials*, vol. 11, no. 1, pp. 116-130, 2009.
- [7] G. Fettweis, M. Krondorf, and S. Bittner, "Gfdm - Generalized Frequency Division Multiplexing," in *Vehicular Technology Conference, 2009. VTC Spring 2009. IEEE 69th*, april 2009, pp. 1-4.
- [8] N. Michailow, M. Lentmaier, P. Rost, and G. Fettweis, "Integration of a Gfdm Secondary System in an Ofdm Primary System," in *Future Network Summit, 2011*, June 2011.
- [9] H. Urkowitz, "Energy detection of unknown deterministic signals," in *Proceedings of the IEEE*, 1967.
- [10] A. Dandawate and G. B. Giannakis, "Statistical tests for presence of cyclostationarity," in *IEEE Trans. Signal Process.*, 1994.
- [11] D. Birru, K. Challapali, and B. Dong, "Detection of the presence of television signals embedded in noise using cyclostationary toolbox," in *US Patent 2010/0157066*, 2010.
- [12] D. Panaitopol, A. Bagayoko, P. Delahaye, and L. Rakotoharison, "Fast and Reliable Sensing Using a Background Process for Noise Estimation," in *In Proc. CrownCom*, 2011.
- [13] H. Ma and J. Wolf, "On Tail Biting Cconvolutional Codes," *IEEE Transactions on Communications*, vol. 34, no. 2, feb. 1986.
- [14] A. Papoulis, "Probability, Random Variables, and Stochastic Processes," in *McGraw-Hill*, 2002.